

WU-B 97-20

July 1997

ELECTROMAGNETIC PROCESSES AND THE DIQUARK MODEL ^a

P. Kroll

Fachbereich Physik, Universität Wuppertal,
D-42097 Wuppertal, Germany

^aInvited talk presented at the Conference on Perspectives in Hadronic Physics, Trieste (May 1997)

ELECTROMAGNETIC PROCESSES AND THE DIQUARK MODEL

PETER KROLL ^b

*Fachbereich Physik, Universität Wuppertal,
D-42097 Wuppertal, Germany*

The present status of the diquark model for exclusive reactions at moderately large momentum transfer is reviewed. That model is a variant of the Brodsky-Lepage approach in which diquarks are considered as quasi-elementary constituents of baryons. Recent applications of the diquark model, relevant to high energy physics with electromagnetic probes, are discussed: electromagnetic form factors of baryons in both the space-like and the time-like region, two-photon annihilations into proton-antiproton pairs as well as real and virtual Compton scattering.

Exclusive processes at large momentum transfer are described in terms of hard scatterings among quarks and gluons ¹. In this so-called hard scattering approach (HSA) a hadronic amplitude is represented by a convolution of process independent distribution amplitudes (DA) with hard scattering amplitudes to be calculated within perturbative QCD. The DAs specify the distribution of the longitudinal momentum fractions the constituents carry. They represent Fock state wave functions integrated over transverse momenta. The convolution manifestly factorizes long (DAs) and short distance physics (hard scattering). The HSA has two characteristic properties, the power laws and the helicity sum rule. The first property says that, at large momentum transfer and large Mandelstam s , the fixed angle cross section of a reaction $AB \rightarrow CD$ behaves as (apart from powers of $\log s$)

$$d\sigma/dt = f(\theta) s^{2-n} \quad (1)$$

where n is the minimum number of external particles in the hard scattering amplitude. The power laws also apply to form factors: a baryon form factor behaves as $1/Q^4$, a meson form factor as $1/Q^2$. The counting rules are found to be in surprisingly good agreement with experimental data. Even at momentum transfers as low as 2 GeV the data seem to respect the counting rules.

The second characteristic property of the HSA is the conservation of hadronic helicity. For a two-body process the helicity sum rule reads

$$\lambda_A + \lambda_B = \lambda_C + \lambda_D. \quad (2)$$

^be-mail: kroll@theorie.physik.uni-wuppertal.de

Supported in part by the TMR Network ERB 4061 PL 95 0115.

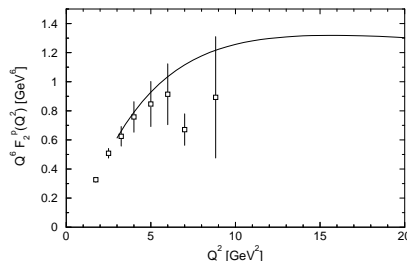


Figure 1: The Pauli form factor of the proton scaled by Q^6 . Data are taken from ². The solid line represents the result obtained with the diquark model ⁷.

It appears as a consequence of utilizing the collinear approximation and of dealing with (almost) massless quarks which conserve their helicities when interacting with gluons. The collinear approximation implies that the relative orbital angular momentum between the constituents has a zero component in the direction of the parent hadron. Hence the helicities of the constituents sum up to the helicity of their parent hadron. The helicity sum rule is violated by 20 – 30% in many cases. A particular striking example is the Pauli form factor of the proton which is determined by a helicity flip contribution. Its Q^2 dependence (see Fig. 1) is compatible with a higher twist contribution ($\sim 1/Q^6$). In explicit applications of the HSA (carried through only in valence quark approximation and to lowest order QCD with very few exceptions) one encounters the difficulty that the data are available only at moderately large momentum transfer, a region in which non-perturbative dynamics may still play a crucial role. A general feature of these applications is the extreme sensitivity of the results to the DAs chosen for the involved hadrons. Only strongly end-point concentrated DAs provide results which are in a few cases in fair agreement with the data ³. These apparent successes of the HSA are only achieved at the expense of strong contributions from soft regions where one of the constituents carries only a tiny fraction of its parent hadron's momentum. This is a very problematical situation for a perturbative calculation. It should be stressed that none of the DAs used in actual applications leads to a successful description of all large momentum transfer processes investigated so far.

It seems clear from the above remarks that the HSA (in the valence quark approximation) although likely to be the correct asymptotic picture for exclusive reactions, needs modifications at moderately large momentum transfer. In a series of papers ^{4–10} such a modification has been proposed by us in which baryons are viewed as composite of quarks and diquarks. The latter are treated as quasi-elementary constituents which partly survive medium hard collisions. Diquarks are an effective description of correlations in the wave

functions and constitute a particular model for non-perturbative effects. The diquark model may be viewed as a variant of the HSA appropriate for moderately large momentum transfer and it is designed in such a way that it evolves into the standard pure quark HSA asymptotically. In so far the standard HSA and the diquark model do not oppose each other, they are not alternatives but rather complements. The existence of diquarks is a hypothesis. However, from experimental and theoretical approaches there have been many indications suggesting the presence of diquarks. For instance, they were introduced in baryon spectroscopy, in nuclear physics, in astrophysics, in jet fragmentation and in weak interactions to explain the famous $\Delta I = 1/2$ rule. Diquarks also provide a natural explanation of the equal slopes of meson and baryon Regge trajectories. For more details and for references, see ⁵. It is important to note that QCD provides some attraction between two quarks in a colour $\{\bar{3}\}$ state at short distances as is to be seen from the static reduction of the one-gluon exchange term.

Even more important for our aim, diquarks have also been found to play a role in inclusive hard scattering reactions. The most obvious place to signal their presence is deep inelastic lepton-nucleon scattering. Indeed the higher twist contributions, convincingly observed by the NMC¹¹, can be modelled as lepton-diquark elastic scattering. Baryon production in inclusive pp collisions also reveals the need for diquarks scattered elastically in the hard interaction¹². For instance, kinematical dependences or the excess of the proton yield over the antiproton yield find simple explanations in the diquark model. No other explanation of these phenomena is known as yet.

The diquark model: As in the standard HSA a helicity amplitude for the reaction $AB \rightarrow CD$ is expressed as a convolution of DAs and hard scattering amplitudes ($s, -t, -u \gg m_i^2$)

$$M(s, t) = \int dx_C dx_D dx_A dx_B \Phi_C^*(x_C) \Phi_D^*(x_D) T_H(x_i, s, t) \Phi_A(x_A) \Phi_B(x_B) \quad (3)$$

where helicity labels are omitted for convenience. Implicitly it is assumed in (3) that the valence Fock states consist of only two constituents, a quark and a diquark (antiquark) in the case of baryons (mesons). In so far the specification of the quark momentum fraction x_i suffices; the diquark (antiquark) carries the momentum fraction $1 - x_i$. If an external particle is point-like, e.g. a photon, the accompanying DA is to be replaced by $\delta(1 - x_i)$. As in the standard HSA contributions from higher Fock states are neglected. This is justified by the fact that such contributions are suppressed by powers of α_s/t as compared to that from the valence Fock state.

In the diquark model spin 0 (S) and spin 1 (V) colour antitriplet diquarks

are considered. Within flavour SU(3) the S diquark forms an antitriplet, the V diquark a sextet. Assuming zero relative orbital angular momentum between quark and diquark and taking advantage of the collinear approximation, the valence Fock state of a ground state octet baryon B with helicity λ and momentum p can be written in a covariant fashion (omitting colour indices)

$$|B; p, \lambda\rangle = f_S \Phi_S^B(x) B_S u(p, \lambda) + f_V \Phi_V^B(x) B_V (\gamma^\alpha + p^\alpha/m_B) \gamma_5 u(p, \lambda) / \sqrt{3} \quad (4)$$

where u is the baryon's spinor. The two terms in (4) represent configurations consisting of a quark and either a scalar or a vector diquark, respectively. The couplings of the diquarks with the quarks in a baryon lead to flavour functions which e.g. for the proton read

$$B_S = u S_{[u,d]} \quad B_V = [u V_{\{u,d\}} - \sqrt{2} d V_{\{u,u\}}] / \sqrt{3}. \quad (5)$$

The DAs $\Phi_{S(V)}^B$ are conventionally normalized as $\int dx \Phi = 1$. The constants f_S and f_V play the role of the configuration space wave functions at the origin. The DAs containing the complicated non-perturbative bound state physics, cannot be calculated from QCD at present. It is still necessary to parameterize the DAs and to fit the eventual free parameters to experimental data. Hence, both the models, the standard HSA as well as the diquark model, only get a predictive power when a number of reactions involving the same hadrons is investigated. In the diquark model the following DAs have been proven to work satisfactorily well in many applications⁷⁻¹⁰:

$$\begin{aligned} \Phi_S^B(x) &= N_S^B x(1-x)^3 \exp[-b^2(m_q^2/x + m_S^2/(1-x))] \\ \Phi_V^B(x) &= N_V^B x(1-x)^3 (1 + 5.8x - 12.5x^2) \exp[-b^2(m_q^2/x + m_V^2/(1-x))]. \end{aligned} \quad (6)$$

The constants N_S^B and N_V^B are fixed through the normalization (e.g. for the proton $N_S^p = 25.97$, $N_V^p = 22.92$). The DAs exhibit a mild flavour dependence via the exponential whose other purpose is to guarantee a strong suppression of the end-point regions. The masses in (6) are constituent masses; for u and d quarks we take 350 MeV and for the diquarks 580 MeV. Strange quarks and diquarks are assumed to be 150 MeV heavier than the non-strange ones. It is to be stressed that the quark and diquark masses only appear in the DAs (6); in the hard scattering kinematics they are neglected. The final results (form factors, amplitudes) depend on the actual mass values mildly. The transverse size parameter b is fixed from the assumption of a Gaussian transverse momentum dependence of the full wave function and the requirement of a value of 600 MeV for the mean transverse momentum (actually $b = 0.498 \text{ GeV}^{-1}$). As the constituent masses the transverse size parameter is not considered as a

free parameter since the final results only depend on it weakly.

The hard scattering amplitudes T_H , determined by short-distance physics, are calculated from a set of Feynman graphs relevant to a given process. Diquark-gluon and diquark-photon vertices appear in these graphs which, following standard prescriptions, are defined as

$$\begin{aligned} \text{SgS} : & \quad i g_s t^a (p_1 + p_2)_\mu \\ \text{VgV} : & \quad -i g_s t^a \left\{ g_{\alpha\beta} (p_1 + p_2)_\mu - g_{\beta\mu} [(1 + \kappa) p_2 - \kappa p_1]_\alpha \right. \\ & \quad \left. - g_{\mu\alpha} [(1 + \kappa) p_1 - \kappa p_2]_\beta \right\} \end{aligned} \quad (7)$$

where $g_s = \sqrt{4\pi\alpha_s}$ is the QCD coupling constant. κ is the anomalous magnetic moment of the vector diquark and $t^a = \lambda^a/2$ the Gell-Mann colour matrix. For the coupling of photons to diquarks one has to replace $g_s t^a$ by $-\sqrt{4\pi\alpha} e_D$ where α is the fine structure constant and e_D is the electrical charge of the diquark in units of the elementary charge. The couplings DgD are supplemented by appropriate contact terms required by gauge invariance.

The composite nature of the diquarks is taken into account by phenomenological vertex functions. Advice for the parameterization of the 3-point functions (diquark form factors) is obtained from the requirement that asymptotically the diquark model evolves into the standard HSA. Interpolating smoothly between the required asymptotic behaviour and the conventional value of 1 at $Q^2 = 0$, the diquark form factors are actually parametrized as

$$F_S^{(3)}(Q^2) = \frac{Q_S^2}{Q_S^2 + Q^2}, \quad F_V^{(3)}(Q^2) = \left(\frac{Q_V^2}{Q_V^2 + Q^2} \right)^2. \quad (8)$$

The asymptotic behaviour of the diquark form factors and the connection to the hard scattering model is discussed in more detail in Ref. ^{5,6}. In accordance with the required asymptotic behaviour the n -point functions for $n \geq 4$ are parametrized as

$$F_S^{(n)}(Q^2) = a_S F_S^{(3)}(Q^2), \quad F_V^{(n)}(Q^2) = \left(a_V \frac{Q_V^2}{Q_V^2 + Q^2} \right)^{n-3} F_V^{(3)}(Q^2). \quad (9)$$

The constants $a_{S,V}$ are strength parameters. Indeed, since the diquarks in intermediate states are rather far off-shell one has to consider the possibility of diquark excitation and break-up. Both these possibilities would likely lead to inelastic reactions. Therefore, we have not to consider these possibilities explicitly in our approach but excitation and break-up lead to a certain amount

of absorption which is taken into account by the strength parameters. Admittedly, that recipe is a rather crude approximation for $n \geq 4$. Since in most cases the contributions from the n -point functions for $n \geq 4$ only provide small corrections to the final results that recipe is sufficiently accurate.

Special features of the diquark model: The diquark hypothesis has striking consequences. It reduces the effective number of constituents inside baryons and, hence, alters the power laws (1). In elastic baryon-baryon scattering, for instance, the usual power s^{-10} becomes $s^{-6}F(s)$ where F represents the net effect of diquark form factors. Asymptotically F provides the missing four powers of s . In the kinematical region in which the diquark model can be applied ($-t, -u \geq 4 \text{ GeV}^2$), the diquark form factors are already active, i.e. they supply a substantial s dependence and, hence, the effective power of s lies somewhere between 6 and 10. The hadronic helicity is not conserved in the diquark model at finite momentum transfer since vector diquarks can flip their helicities when interacting with gluons. Thus, in contrast to the standard HSA, spin-flip dependent quantities like the Pauli form factor of the nucleon can be calculated.

Electromagnetic nucleon form factors: This is the simplest application of the diquark model and the most obvious place to fix the various parameters of the model. The Dirac and Pauli form factors of the nucleon are evaluated from the convolution formula (3) with the DAs (6) and the parameters are determined from a best fit to the data in the space-like region. The following set of parameters

$$\begin{aligned} f_S &= 73.85 \text{ MeV}, & Q_S^2 &= 3.22 \text{ GeV}^2, & a_S &= 0.15, \\ f_V &= 127.7 \text{ MeV}, & Q_V^2 &= 1.50 \text{ GeV}^2, & a_V &= 0.05, & \kappa &= 1.39; \end{aligned} \quad (10)$$

provides a good fit of the data⁷. α_s is evaluated with $\Lambda_{QCD} = 200 \text{ MeV}$ and restricted to be smaller than 0.5. The parameters Q_S and Q_V , controlling the size of the diquarks, are in agreement with the higher-twist effects observed in the structure functions of deep inelastic lepton-hadron scattering¹¹ if these effects are modelled as lepton-diquark elastic scattering. The Dirac form factor of the proton is perfectly reproduced. The results for the Pauli form factor are shown in Fig. 1. The predictions for the two neutron form factors are also in agreement with the data. However, more accurate neutron data are needed in the Q^2 region of interest in order to determine the model parameters better. The nucleon's axial form factor⁷ and its electromagnetic form factors in the time-like regions⁸ have also been evaluated. Both the results compare well with data. Even electroexcitation of nucleon resonances has been investigated^{13,14}. In the case of the $N\Delta$ form factor the model results agree very well with recent data¹⁵.

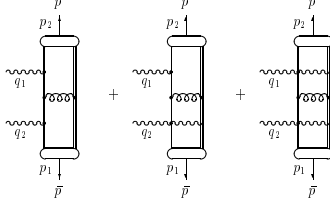


Figure 2: Typical Feynman graphs contributing to $\gamma^{(*)} p \rightarrow \gamma p$.

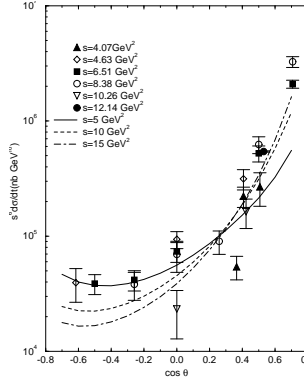


Figure 3: The scaled cross section for RCS off protons vs. $\cos \theta$ for three different photon energies. The experimental data are taken from ¹⁶.

Real Compton scattering (RCS): $\gamma p \rightarrow \gamma p$ is the next reaction to which the diquark model is applied to. Since the only hadrons involved are again protons RCS can be predicted in the diquark model without any adjustable parameter. Typical Feynman graphs contributing to that process are shown in Fig. 2. The results of the diquark model for RCS are shown in Fig. 3 for three different photon energies ^{6,9}. Note that in the very forward and backward regions the transverse momentum of the outgoing photon is small and, hence, the diquark model which is based on perturbative QCD, is not applicable. Despite the rather small energies at which data ¹⁶ are available, the diquark model is seen to work rather well. The predicted cross section does not strictly scale with s^{-6} . The results obtained within the standard HSA are of similar quality ¹⁷. The diquark model also predicts interesting photon asymmetries and spin correlation parameters (see the discussion in ⁶). Even a polarization of the proton, of the order of 10%, is obtained ⁶. This comes about as a consequence of helicity flips generated by vector diquarks and of perturbative phases produced

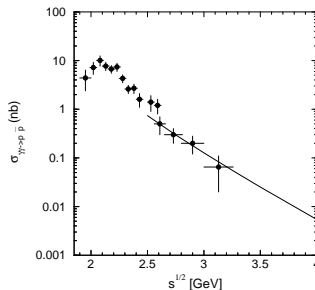


Figure 4: The integrated $\gamma\gamma \rightarrow p\bar{p}$ cross section ($|\cos\theta| \geq 0.6$). The solid line represents the diquark model prediction⁸. Data are taken from CLEO¹⁹.

by propagator poles appearing within the domains of the momentum fraction integrations. The poles are handled in the usual way by the $i\varepsilon$ prescription. The appearance of imaginary parts to leading order of α_s is a non-trivial prediction of perturbative QCD¹⁸; it is characteristic of the HSA and is not a consequence of the diquark hypothesis.

Two-photon annihilation into $p\bar{p}$ pairs: This process is related to RCS by crossing, i.e. the same set of Feynman graphs contributes (see Fig. 2). The only difference is that now the diquark form factors are needed in the time-like region. The expressions (8,9) represent an effective parameterization of them valid at space-like Q^2 . Since the exact dynamics of the diquark system is not known it is not possible to continue these parameterizations to the time-like region in a unique way. A continuation can be defined as follows⁸: Q^2 is replaced by $-s$ in (8,9) guaranteeing the correct asymptotic behaviour and, in order to avoid the appearance of unphysical poles at low Q^2 , the diquark form factors are kept constant once their absolute values have reached $c_0 = 1.3$ ⁸. The same definition of the time-like diquark form factors is used in the analysis the proton form factor in the time-like region. The diquark model predictions for the integrated $\gamma\gamma \rightarrow p\bar{p}$ cross section is compared to the CLEO data¹⁹ in Fig. 4. At large energies the agreement between predictions and experiment is good. The predictions for the angular distributions are in agreement with the CLEO data too. The standard HSA on the other hand predicts a cross section which lies about an order of magnitude below the data²⁰. Recently CLEO has also measured two-photon annihilations into $\Lambda\bar{\Lambda}$ pairs²¹. At large energies the integrated $\Lambda\bar{\Lambda}$ cross section is about a factor of 2 smaller than that one for annihilations into $p\bar{p}$ pairs. This may be taken as a hint at a more complicated Λ wave function than (4,6).

Virtual Compton scattering (VCS): This process is accessible through $ep \rightarrow ep\gamma$. An interesting element in that reaction is that, besides VCS, there is also a contribution from the Bethe-Heitler (BH) process where the final state photon is emitted from the electron. Electroproduction of photons offers many possibilities to test details of the dynamics: One may measure the s , t and Q^2 dependence as well as that on the angle ϕ between the hadronic and leptonic scattering planes. This allows to isolate cross sections for longitudinal and transverse virtual photons. One may also use polarized beams and targets and last but not least one may measure the interference between the BH and the VC contributions. The interference is sensitive to phase differences.

At s , $-t$ and $-u \gg m_p^2$ (or small $|\cos\theta|$ where θ is the scattering angle of the outgoing photon in the photon-proton center of mass frame) the diquark model can also be applied to VCS⁹. Again there is no free parameter in that calculation. The relevant Feynman graphs are the same as for RCS (see Fig. 2). The model can safely be applied for $s \geq 10 \text{ GeV}^2$ and $|\cos\theta| \leq 0.6$. For the future CEBAF beam energy of 6 GeV the model is at its limits of applicability. However, since the diquark model predictions for real Compton scattering do rather well agree with the data even at $s \geq 5 \text{ GeV}^2$ (see Fig. 3) one may expect similarly good agreement for VCS. Predictions for the VCS cross section are given in⁹. The transverse cross section (which, at $Q^2 = 0$, is the cross section for RCS) is the dominant piece. The other cross sections only become sizeable for larger values of $|\cos\theta|$. Examination of the Bethe-Heitler contribution to the process $ep \rightarrow ep\gamma$ reveals that it is small as compared to the VCS contribution at high energies, small values of $|\cos\theta|$ and for an out-of-plane experiment, i.e. $\phi \geq 50^\circ$.

Of interest is also the electron asymmetry in $ep \rightarrow ep\gamma$:

$$A_L = \frac{\sigma(+) - \sigma(-)}{\sigma(+) + \sigma(+)} \quad (11)$$

where \pm indicates the helicity of the incoming electron. A_L measures the imaginary part of the longitudinal – transverse interference. The longitudinal amplitudes for VCS turn out to be small in the diquark model (hence A_L^{VC} is small). However, according to the model, A_L is large in the region of strong BH contamination (see Fig. 5). In that region, A_L measures the relative phase (being of perturbative origin from on-shell going internal gluons, quarks and diquarks¹⁸) between the BH amplitudes and the VCS ones. The magnitude of the effect shown in Fig. 5 is sensitive to details of the model and, therefore, should not be taken literally. Despite of this our results may be taken as an example of what may happen. The measurement of A_L , e.g. at CEBAF, will elucidate the underlying dynamics of VCS strikingly.

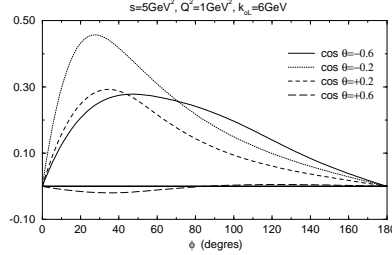


Figure 5: Diquark model predictions for the electron asymmetry in $ep \rightarrow ep\gamma$.

Summary and outlook: The diquark model which represents a variant of the HSA, combines perturbative QCD with non-perturbative elements. The diquarks represent quark-quark correlations in baryon wave functions which are modelled as quasi-elementary constituents. This model has been applied to many photon induced exclusive processes at moderately large momentum transfer (typically $\geq 4 \text{ GeV}^2$). From the analysis of the nucleon form factors the parameters specifying the diquark and the DAs, are fixed. Compton scattering and two-photon annihilations of $p\bar{p}$ can then be predicted. The comparison with existing data reveals that the diquark model works quite well and in fact much better than the pure quark HSA.

Predictions for the VCS cross section and for the $ep \rightarrow ep\gamma$ cross section have also been made for kinematical situations accessible at the upgraded CEBAF and perhaps at future high energy accelerators like ELFE@HERA. According to the diquark model the BH contamination of the photon electroproduction becomes sizeable for small azimuthal angles. The BH contribution also offers the interesting possibility of measuring the relative phases between the VC and the BH amplitudes. The phases of the VC amplitudes are a non-trivial phenomenon generated by the fact that some of the internal quarks, diquarks and gluons may go on mass shell. The electron asymmetry A_L is particularly sensitive to relative phases. In contrast to the standard HSA the diquark model allows to calculate helicity flip amplitudes, the helicity sum rule (2) does not hold at finite Q^2 . One example of an observable controlled by helicity flip contributions is the Pauli form factor of the proton. Also in this case the diquark model accounts for the data.

Photo- and electroproduction of mesons can also be calculated within the diquark model. However, these reactions are already quite complicated since all together 158 Feynman graphs contribute. The analysis of this class of processes is not yet finished. First results exist only for $\gamma p \rightarrow K^{(*)}\Lambda$ ¹⁰.

The only discrepancy between data and diquark model predictions known to

us, is to be seen in the process $\gamma\gamma \rightarrow \Lambda\bar{\Lambda}$. This failure seems to indicate that the Λ wave function, and perhaps those of other hyperons are more complicated than (4,6). A solution of this problem may necessitate a combined analysis of $\gamma\gamma \rightarrow \Lambda\bar{\Lambda}$ and $\gamma p \rightarrow K^{(*)}\Lambda$.

References

1. G.P. Lepage and S.J. Brodsky, *Phys. Rev. D* **22**, 2157 (1980).
2. P. Bosted et al., *Phys. Rev. Lett.* **68**, 3841 (1992).
3. V.L. Chernyak and A.R. Zhitnitsky, *Phys. Rep.* **112**, 173 (1984).
4. M. Anselmino, P. Kroll and B. Pire, *Z. Phys. C* **36**, 89 (1987).
5. P. Kroll, Proceedings of the Adriatico Research Conference on Spin and Polarization Dynamics in Nuclear and Particle Physics, Trieste, 1988.
6. P. Kroll, W. Schweiger and M. Schürmann, *Int. Jour. of Mod. Physics A* **6**, 4107 (1991).
7. R. Jakob, P. Kroll, M. Schürmann and W. Schweiger, *Z. Phys. A* **347**, 109 (1993).
8. P. Kroll, Th. Pilsner, M. Schürmann and W. Schweiger, *Phys. Lett. B* **316**, 546 (1993).
9. P. Kroll, M. Schürmann and P. Guichon, *Nucl. Phys. A* **598**, 435 (1996).
10. P. Kroll, M. Schürmann, K. Passek and W. Schweiger, *Phys. Rev. D* **55**, 4315 (1997).
11. M. Virchaux and A. Milsztajn, *Phys. Lett. B* **274**, 221 (1992).
12. A. Breakstone et al., *Z. Phys. C* **28**, 335 (1985).
13. P. Kroll, M. Schürmann and W. Schweiger, *Z. Phys. A* **342**, 429 (1992).
14. J. Bolz, P. Kroll and J.G. Körner, *Z. Phys. A* **350**, 145 (1994).
15. L.M. Stuart et al, hep-ph/9612416, submitted to *Phys. Rev. D*.
16. M.A. Shupe et al., *Phys. Rev. D* **19**, 1921 (1979).
17. A.S. Kronfeld and B. Nžić, *Phys. Rev. D* **44**, 3445 (1991).
18. G.R. Farrar et al., *Phys. Rev. Lett.* **62**, 2229 (1989).
19. M. Artuso et al., CLEO collaboration, *Phys. Rev. D* **50**, 5484 (1994).
20. G.R. Farrar, E. Maina and F. Neri, *Nucl. Phys. B* **259**, 702 (1985); *B* **263**, 746 (1986)(E).
21. S. Anderson et al., CLEO collaboration, hep-ex/9701013.
22. R.L. Anderson et al., *Phys. Rev. D* **14**, 679 (1976).
23. G.R. Farrar, K. Huleihel and H. Zhang, *Nucl. Phys. B* **349**, 655 (1991).